Hyperfine Interact
DOI 10.1007/s10751-013-0863-0

Mössbauer and vibrational DOS studies of diluted magnetic tin oxides and nano iron oxides

K. Nomura · A. I. Rykov · A. M. Mudarra Navarro · C. E. Rodriguez Torres · L. A. Errico · C. A. Barrero · Y. Yoda

Abstract The magnetic properties and Mössbauer results for SnO_2 doped with ^{57}Fe are reviewed, and the values of isomer shift and quadrupole splitting are compared with the results obtained by *ab initio* calculations. It is concluded that the exchange interactions between oxygen defects and magnetic atoms are responsible for long range magnetic interactions of dilute Fe ions dispersed in SnO_2. Fe atom precipitated clusters may be formed in highly Fe doped SnO_2 samples by annealing at relatively high temperatures for several hours. The reduction of the particle size to nano-scale dimensions induces magnetization, which can be associated with oxygen defects. We have measured the nuclear inelastic scattering (NIS) spectra of Fe oxides, and ^{57}Fe and (Co or Mn) doped SnO_2 synthesized mainly by sol–gel methods and we have derived the vibration density of states (VDOS). The local phonons are sensitive to the presence of precipitated clusters.

Proceedings of the Thirteenth Latin American Conference on the Applications of the Mössbauer Effect (LACAME 2012), Medellín, Colombia, 11–16 November 2012.

K. Nomura (✉) · A. I. Rykov
School of Engineering, The University of Tokyo, Tokyo, Japan
e-mail: k-nomura@t-adm.t.u-tokyo.ac.jp, dqf10204@nifty.com

A. I. Rykov
Mössbauer Effect Data Centre, Dalian, China

A. M. Mudarra Navarro · C. E. Rodriguez Torres · L. A. Errico
Universidad Nacional de La Plata, La Plata, Argentina

C. A. Barrero
University of Antioquia, Madellín, Colombia

Y. Yoda
Japan Synchrotron Radiation Research Institute, Hyogo, Japan

Published online: 18 April 2013

Keywords Vibration DOS · Iron doped tin oxides · Diluted magnetic oxides · Nuclear inelastic scattering · Mössbauer · $MnFe_2O_4$ · $CoFe_2O_4$ · Mn and Fe co-doped SnO_2 · Co and Fe co-doped SnO_2

1 Introduction

^{57}Fe atoms are magnetic and can be used as Mössbauer nuclear probes. Recently, oxide semiconductors doped with magnetic atoms have excited much interest in issues of both applied spintronics and basic physics of diluted magnetic atoms acquiring a larger magnetic moment with decreasing magnetic atom concentration. Dielt et al. predicted that transparent semiconductors with wide bandgap such as ZnO and GaN become ferromagnetic at room temperature (RT) by doping with dilute magnetic atoms [1]. Chemically synthesized powders of SnO_2 doped with Co and Fe have been studied by Punnoose et al. [2, 3], and Hays et al. [4]. The authors suggested a close relationship between the structural and magnetic properties in Fe-doped SnO_2 nano-scale particles. In all of these works, the observed ferromagnetism has been attributed to interaction between the magnetic impurities, but the main source of the observed ferromagnetism has never been associated with magnetically ordered defects yet. It was reported that when oxygen vacancies near Fe atom are introduced, the magnetic moment increases [5]. Several kinds of Fe states were identified by synthesizing SnO_2 doped with ^{57}Fe using a sol gel method [6].

The ferromagnetism of SnO_2 doped with Fe is presumed to be induced either by the spin ordering of magnetic atoms through localized spins trapped at oxygen defects or by the formation of precipitated magnetic clusters [6]. It is necessary to reveal how the ferromagnetic atoms, either dispersed or clustered, are incorporated inside the SnO_2 semiconductor, and how Fe ions substitutionally located at Sn site interact with the oxygen vacancies. Magnetism in diluted magnetic semiconductors (DMS) has been considered by some theories to be induced by the RKKY interaction, or carrier-induced interaction between magnetic ions [7–9], or by impurity band exchange interaction, which implies that the magnetic moments are hybridized under the conduction band [10], or by the large polaron model of magnetism mediated by defects [11].

Sb and Fe co-doping of SnO_2 increases its electrical conductivity and induces magnetism. The doping by Sb ions induces a higher solubility of Fe ions in SnO_2, and magnetization of cassiterite based materials increases with Fe concentration [12]. The doping effects of non magnetic Zn ions were also studied for Fe and Sb doped SnO_2. It was found that the saturation magnetization increases with the addition of less than 10 % of non-magnetic Zn ions [13], and that Fe and Co [14, 15] (Fe and Mn [16], or Fe and Ni [17]) co-doped SnO_2 gave rise to enhanced magnetization as compared with the single atom doped SnO_2. In the case of diluted ^{57}Fe substituted at the Sn site in SnO_2 obtained by a sol–gel method, the experimental Mössbauer parameters were compared with *ab initio* calculations [18] to determine the local structure around iron in SnO_2 rutile structure.

On the other hand, a nuclear resonance inelastic scattering (NIS) spectrum can be obtained due to the annihilation and creation of vibration energy quanta at both sides of the nuclear resonance elastic scattering peak. As a supplementary analysis, it is important to measure the NIS spectra of various iron oxides, which may be precipitated by synthesis and annealing.

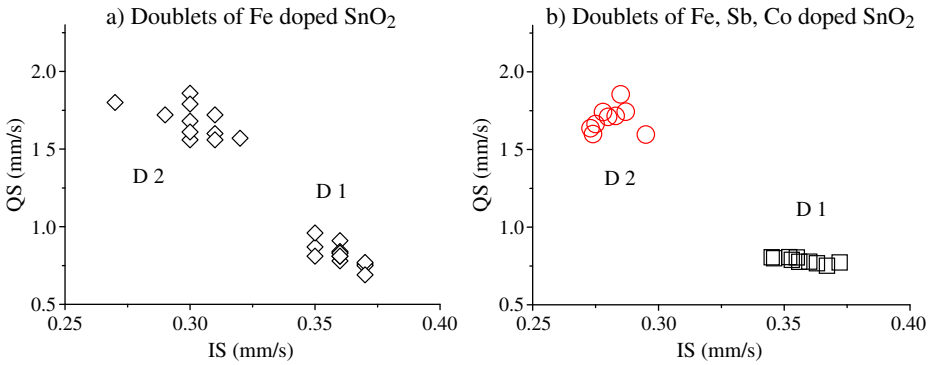

Fig. 1 Relationship between IS and QS values on Fe doped SnO_2 [6] and Fe, Co, Sb co-doped SnO_2 [20]

2 Experimental

^{57}Fe doped $SnO_{2-\delta}$, Fe oxides, (Fe, Mn) oxides, and (Fe, Co) oxides were obtained by a sol–gel method [6]. Only γ-Fe_2O_3 was donated by Toda Kogyo Corporation. Mössbauer spectra were measured by a conventional transmission method with velocity calibration by α-Fe. NIS spectra were measured using the BL09 beam with energy resolution of 2.5 meV in the synchrotron facility of SPring8. While the incidence energy of 14.41 keV was modulated from −80 meV to +80 meV, the NIS spectra were measured several times by detecting the scattered resonant X-rays after Mössbauer effect with APD detectors. Vibration densities of states (VDOS) were derived from the NIS spectra [19].

3 Results

3.1 Mössbauer parameters and oxygen vacancy

Figure 1 shows the relationship between isomer shift (IS) and quadrupole splitting (QS) values in two doublets, observed in the Mössbauer spectra of Fe doped SnO_2 [6] and (Fe, Co and Sb) doped SnO_2 [20], respectively. Fe-doped SnO_2 has a major doublet 1 (D1) with IS values of 0.34–0.37 mm/s and QS values of 0.5–0.9 mm/s, and a minor doublet 2 (D2) with IS = 0.29–0.34 mm/s and QS = 1.5–1.8 mm/s. (Fe, Co, Sb) co-doped SnO_2 has D1 with IS = 0.34–0.37 mm/s and QS = 0.7–0.8 mm/s, and D2 with IS = 0.27–0.29 mm/s and QS = 1.6–1.8 mm/s. Both doublets correspond to Fe (III). The IS values of D2 for the group of (Fe, Co, Sb) doped SnO_2 are relatively smaller than those of D2 for SnO_2 only doped with Fe, which show a relatively large distribution. On the other hand, the magnetic hysteresis for (Fe, Co, and Sb) doped SnO_2 is broader than that of Fe-doped SnO_2. The relative fraction of D2 decreases with the increase of Sb doping rate, whereas the proportion of the broad sextet increases with the increase of Fe concentration [20].

According to our *ab initio* calculations [18] the hyperfine parameters for D2 are close to the calculated ones for the model of Fe substituting Sn in the rutile structure

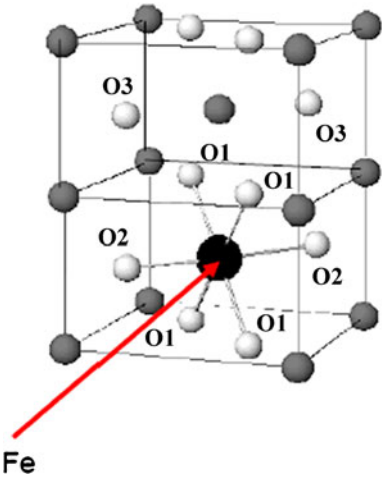

Fig. 2 The structure of SnO_2 with the substituted Fe and different types of oxygen vacancies as explained in the text

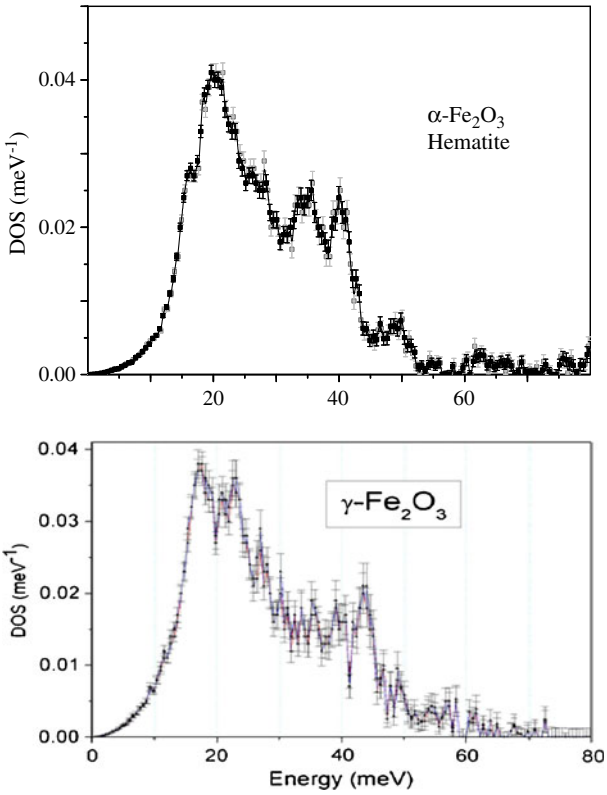

Fig. 3 Vibration DOS of hematite (α-Fe_2O_3), and maghemite (γ-Fe_2O_3)

with an oxygen vacancy at O2 (apical oxygen of the octahedron, see Fig. 2). In this case the calculated values are: IS = 0.32 and QS = 1.43 mm/s. The experimental values are also in agreement with the model where two iron atoms substitute tin atoms, one in the centre and the other in a corner of unit cell sharing an oxygen

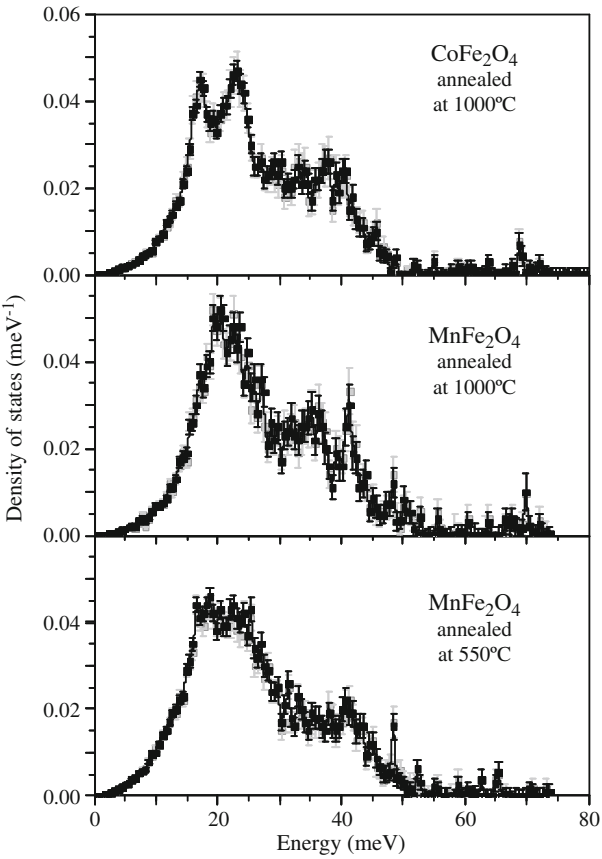

Fig. 4 Vibration DOS of Co ferrite and Mn ferrite: **a** $CoFe_2O_4$ annealed at 1,000 °C, **b** $MnFe_2O_4$, annealed at 1,000 °C, and $MnFe_2O_4$ annealed at 550 °C

vacancy. In this case the calculation predicts the existence of two non-equivalent iron atoms with hyperfine parameters: $IS_1 = 0.32$ and $QS_1 = 1.30$ mm/s and $IS_2 = 0.31$ and $QS_2 = 2.03$ mm/s, respectively.

In the case of doublet D1, the experimental values are between the calculated ones for the model of iron substituting Sn with an oxygen vacancy at O1 (basal plane of the octahedron, see Fig. 2) and the model of two iron substituting tin central atom of the unit cell along the c-axis that share an oxygen vacancy at O1. The calculated hyperfine parameters for these configurations are: IS = 0.48 mm/s and QS = 0.92 mm/s (for one iron with vacancy at O1) and IS = 0.35 mm/s and QS = 0.51 mm/s (for two irons sharing an oxygen vacancy at O1).

Interstitial Fe sites cannot be responsible for the observed hyperfine interaction data because the calculated IS values (between 0.5 and 0.7 mm/s) are larger than the experimental ones.

We can therefore conclude that the experimental values of hyperfine parameters are consistent with iron substituting tin in the rutile structure associated with oxygen vacancies near iron impurities.

A magnetic sextet with IS = 0.37 mm/s and H = 51 T was also observed, and it can be associated with hematite precipitated in the SnO_2 matrix. The hematite contains Sn atoms because the Morin transition was not observed at low temperature [12]. In

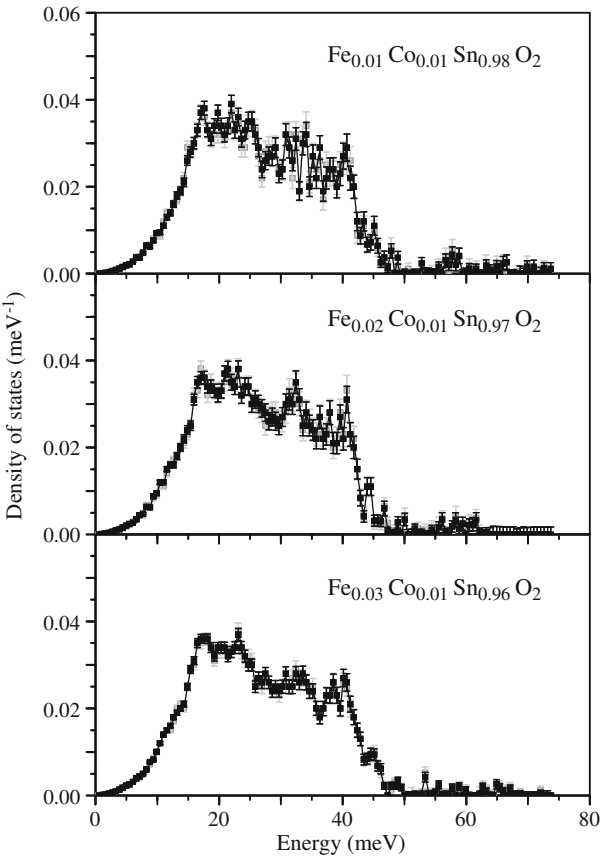

Fig. 5 VDOS of SnO_2 doped with Fe and Co. Average crystallite size: 46 nm, 43 nm, and 36 nm of SnO_2 for 1 %Fe + 1 %Co doped SnO_2, 2 %Fe + 1 %Co doped SnO_2, and 3 %Fe + 1 %Co doped SnO_2, respectively

addition to the sextet with 51 T, another broad sextet with H = 49 T was observed. We are uncertain whether or not this sextet is caused by precipitates of maghemite.

In the case of highly Fe doped SnO_2, and two TMs co-doped SnO_2, it can be considered that the magnetism originates not only from the impurity clustering but also from double exchange interactions of dispersed Fe(III) and TM(II) mediated by oxygen defects produced at the interface of a cluster or at a grain boundary. It is known that point defects like *F* centers, which consist of two adjacent singly occupied vacancies, can also be ferromagnetically ordered [21]. Now, it was observed that the shape of the low temperature Mössbauer spectra did not noticeably change with respect to the room temperature spectrum. These data suggest that the relaxation can be originating from weakly interacting magnetic polarons or small size polaron clusters. Bergqvist et al. [22] have proposed that the magnetic ordering in DMS materials is greatly affected by magnetic percolation, and that the main source of ferromagnetism comes from the short range interatomic exchange interactions that are strongly localized in real space. Moreover, it is also possible that magnetic defects can be also contributing to the magnetization value. Therefore, the interface defects between clusters and host matrix oxide are considered to be an important source of magnetism.

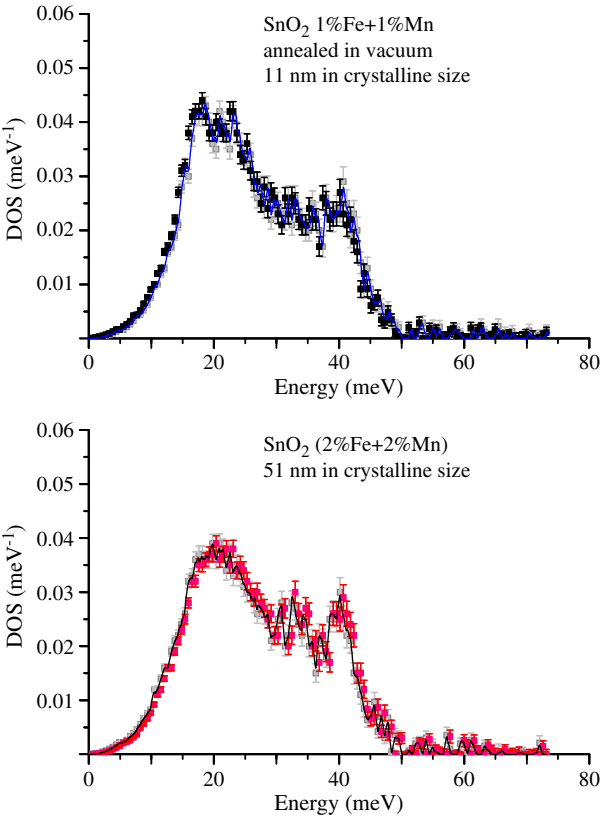

Fig. 6 VDOS of SnO_2 doped with Fe and Mn (Doping rate: 1 % Fe + 1 % Mn, 2 % Fe + 2 % Mn)

3.2 VDOS of Fe doped SnO_2 and ferrite oxides

The oxides SnO_2(Fe), γ-Fe_2O_3, α-Fe_2O_3, $CoFe_2O_4$, and $MnFe_2O_4$ were measured by NIS. Figure 3 shows VDOS of α-Fe_2O_3 and γ-Fe_2O_3. The corundum structure of α-Fe_2O_3 showed particular phonon peaks at 16, 21, 27, 35, 40 and 49 meV, whereas the inverse spinel structure of γ-Fe_2O_3 shows particular peaks at 18, 23, 27, 35, 39, 44, and 50 meV.

VDOS of the inverse spinel structures of $CoFe_2O_3$, and $MnFe_2O_3$, prepared by a sol–gel method and treated at different annealing temperatures, are shown in Fig. 4. The main peaks are around 17, 23, 38, and 40 meV for $CoFe_2O_3$, whereas the peaks are at 20, 23, 35, and 42 meV for $MnFe_2O_3$ annealed at 1,000 °C, and at 18, 23, 43 meV for $MnFe_2O_3$ annealed at 550 °C. Phonon softening is observed for $MnFe_2O_3$ annealed at low temperatures. It is believed to be due to the low degree of crystallinity. The inverse spinel type of ferrites show similar VDOS'es, which may be somewhat influenced by the amount of Fe(III) ions occupied at tetrahedral and octahedral sites.

Figure 5 shows the VDOS of SnO_2 doped with 1 %, 2 % or 3 %Fe and 1 %Co. With increasing Fe contents, a shoulder appears at the energies lower than 15 meV. The typical shapes at larger energies are similar to those of a ferrite, although VDOS of SnO_2 also shows a somewhat similar shape [23]. It may suggest that some spinel-type of Fe and Co compounds cannot be excluded. In contrast, from the VDOS

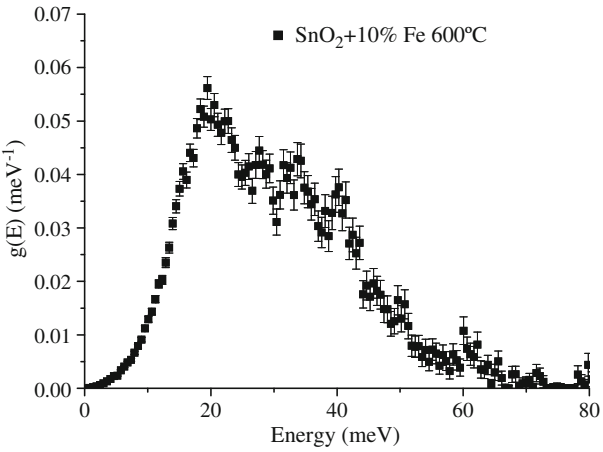

Fig. 7 VDOS of 10 % Fe doped SnO_2 annealed at 600 °C

results, pure α-Fe_2O_3 is excluded. It has a peak at 49 meV, which is not observed elsewhere. The VDOS distribution of SnO_2 doped with Fe and Co are observed below 47 meV as shown in Fig. 5.

The VDOS of SnO_2 doped with Fe and Mn looks more similar to that of SnO_2 doped with Fe as shown in Fig. 6. If the small clusters of Fe oxides are precipitated in SnO_2, the distribution of VDOS spreads to low energy and high energy regions as shown in Fig. 7. In this case, the crystallites of SnO_2 are characterized by a small size, giving rise to the VDOS enhancement. The VDOS in lower energy regions is enhanced for (Fe, Co) doped SnO_2 and (Fe, Mn) co-doped SnO_2.

The precipitated Fe compound cannot be clearly identified but the composition of the small clusters might be derived from the VDOS. There is a possibility that small clusters such as $CoFe_2O_4$ and $MnFe_2O_4$ are formed in several 10 nm crystalline SnO_2, although XRD could not detect those compounds.

4 Summary

Two doublets and sextets with sharp and broad relaxation peaks have been observed in Mössbauer spectra of Fe doped and two transition metal co-doped SnO_2. It is clear from *ab initio* calculations that when Fe(III) is located at Sn site of SnO_2, one oxygen vacancy is created. One doublet (D1) is due to Fe (III) with one oxygen vacancy in the basal plane of the octahedron. The other doublet (D2) is due to Fe(III) with an oxygen vacancy in the vertex of the octahedron, or with two substitutional Fe(III), between which one oxygen is vacant. The sextet with sharp peaks is due to α-Fe_2O_3 with $H = 51$ T. The saturation magnetization is enhanced for (Fe, Co) co-doped SnO_2 [14] or (Fe, Mn) co-doped SnO_2 [16], in contrast to single metal ion doped SnO_2. The broad sextet with 47–49 T cannot be assigned uniquely although it may be identified either with a large magnetic polaron or with γ-Fe_2O_3.

In this paper, (Co, Fe) and (Mn, Fe) ferrite oxides and dilute (Fe, Co) or (Fe, Mn) co-doped SnO_2 were prepared by a sol–gel method and measured by NIS to obtain the VDOS. It is concluded from VDOS that clusters may be formed in (Fe, Co) or (Fe, Mn) co-doped SnO_2 with highly doping.

References

1. Dielt, T., Ohno, H., Matsukura, F.: Phys. Rev. B **63**, 195205 (2001)
2. Punnoose, A., Hays, J., Gopal, V., Shutthanandan, V.: Appl. Phys. Lett. **85**, 1559 (2004)
3. Punnoose, A., Hays, J., Thurber, A., Engelhard, M.H., Kukkadapu, R.K., Wang, C., Shutthanandan, V., Thevuthasan, S.: Phys. Rev. B **72**, 54402 (2005)
4. Hays, J., Punnoose, A., Baldner, R., Engelhard, M.H., Peloquin, J., Reddy, K.M.: Phys. Rev. B **72**, 75203 (2005)
5. Rodriguez Torres, C.E., Errico, L., Golmar, F., Mudarra Navarro, A.M., Cabrera, A.F., Duhalde, S., Sanchez, F.H., Weissmann, M.: J. Magn. Magn. Mater. **316**, e219 (2007)
6. Nomura, K., Barrero, C., Sakuma, J., Takeda, M.: Phy. Rev. B **75**, 184411 (2007)
7. Ruderman, M.A., Kittel, C.: Phys. Rev. **96**, 99 (1954)
8. Kasuya, T.: Prog. Theor. Phys. **16**, 45 (1956)
9. Yosida, K.: Phys. Rev. **106**, 893 (1957)
10. Coey, J.M., Douvalis, A.P., Fitzgerald, C.B., Venkatesan, M.: Appl. Phys. Lett. **84**, 1332 (2004)
11. Coey, J.M., Venkatesan, M., Stamenov, P., Fitzgerald, C.B., Dorneles, L.S.: Phys. Rev. B **72**, 24450 (2005)
12. Nomura, K., Barrero, C.A., Kuwano, K., Yamada, Y., Saito, T., Kuzmann, E.: Hyperfine Interact. **191**, 25 (2009)
13. Nomura, K., Rykov, A., Nemeth, Z., Yoda, Y.: Hyperfine Interact. **205**, 129 (2012)
14. Nomura, K., Okabayashi, J., Okamura, Yamada, Y.: J. Appl. Phys. **110**, 83901 (2011)
15. Kono, S., Nomura, K., Yamada, Y., Okabayashi, J.: Hyperfine Interact. **205**, 105 (2012)
16. Okabayashi, J., Nomura, K., Kano, S., Yamada, Y.: Jpn. J. Appl. Phys. **51**, 23003 (2012)
17. Okabayashi, J., Kono, S., Yamada, Y., Nomura, K.: J. Appl. Phys. **112**, 73917 (2012)
18. Mudarra Navarro, A.M., Rodriguez Torres, C.E., Errico, L.A.: in private communication
19. Rykov, A.I., Nomura, K., Mitsui, T., Seto, M.: Physica B **350**, 287 (2004)
20. Nomura, K., Shima, A.: AIP Conf. Proc. (MSMS2012) **1489**, 13 (2012)
21. Stoneham, A.M.: Theory of Defects in Solids, chap. 14. Clarendon Press, Oxford (1975)
22. Bergqvist, L., Eriksson, O., Kudrnovsky, J., Drchal, V., Korzhavyi, P., Turek, I.: Phys. Rev. Lett. **93**, 137202 (2004)
23. Rykov, A.I., Nomura, K., Sakuma, J., Barrero, C., Yoda, Y., Mitsui, T.: Phys. Rev. B **77**, 014302 (2008)